Membrane remodeling due to mixture of multiple types of curvature proteins

Gaurav Kumar[1] and Anand Srivastava[1, a)]

Molecular Biophysics Unit, Indian Institute of Science Bangalore,

C. V. Raman Road, Bangalore, Karnataka 560012, India

Abstract: We present an extension of the Monte Carlo based mesoscopic membrane model, where the membrane is represented as a dynamically triangulated surface and the proteins are modeled as anisotropic inclusions formulated as in-plane nematic field variables adhering to the deformable elastic sheet. In the extended model, we have augmented the Hamiltonian to study membrane deformation due to a mixture of multiple types of curvature generating proteins. This feature opens the door for understanding how multiple kinds of curvature-generating proteins may be working in a coordinated manner to induce desired membrane morphologies. For example, among other things, we study membrane deformations and tubulation due to a mixture of positive and negative curvature proteins as mimics of various proteins from BAR domain family working together for curvature formation and stabilization. We also study the effect of membrane anisotropy, which manifests as membrane localization and differential binding affinity of a given curvature protein, leading to insights into the tightly regulated cargo sorting and transport processes. Our simulation results show different morphology of deformed vesicles that depend on the curvatures and densities of the participating proteins as well as on the protein-protein and membrane-proteins interactions.

Significance: Membrane remodeling requires highly orchestrated interactions between several types of lipids and curvature proteins. Experimentally probing the membrane deformation intermediates is non-trivial. For example, it is not known exactly how two or more different kinds of BAR domain proteins work in concert to induce and stabilize certain membrane curvatures. In this work, we use mesoscopic continuum modeling and explore the factors that induce and stabilize a range of membrane deformation due to a mixture of positive and negative curvature proteins.

Keywords Curvature proteins, Membrane Remodelling, Protein-protein interactions, Mesoscopic Modeling, Helfric Hamiltonian

[a)] Electronic mail: anand@iisc.ac.in

I. INTRODUCTION

Bio-molecular structures dynamically assemble, perform highly orchestrated biochemical functions, and disassemble seamlessly before reassembling to continue the cycle. Since the molecular structure and the biochemical pathways in biological processes are optimized over evolutionary timescales to perform elaborate functions, the "biological circuitry" is extremely sophisticated. Despite being under strong thermal noise and embedded in a crowded molecular milieu, the molecular machines and motors encrypt and process complex set of information in a precise manner. This information is embedded at multiple length and time scales that range from structures at atomic resolution to formation of molecular complexes and leading to subcellular and cellular processes such as ion transport across channels and pumps, fusion and fission in endocytic recycling, presynaptic neurotransmission, morphogenesis and metastasis to name a few[1–3].

A paradigmatic example of this "biological circuitry" is the Clathrin-mediated endocytosis (CME) in vesicular trafficking. After five decades since its discovery in 1964 and countless seminal subsequent discoveries, it is now well established that more than 50 proteins make up this molecular machinery[4–6]. Proteins, either individually or in complex are "called upon" from the cytosolic reservoir in a highly coordinated manner at different stages that include (i) initiation/identification of the endocytic site, (ii) recruitment of the cargo to the site, (iii) invagination/remodelling of the membrane, (iv) leakage-free scission (v) disassembly/uncoating of proteins and (vi) vesicle release for trafficking. These functions are carried out by disparate proteins that have been studied in great detail. However, we still lack a good understanding of how all these different components work together in a highly coordinated manner to drive vesicle formation. There are several examples like CME in the cell, which take place due to a large number of proteins and other biomolecules working as a 'biological circuitry'.

BAR domain class of proteins are the quintessential curvature inducing scaffold proteins and are ubiquitously present in the endocytic recycling pathways and play a crucial role in vesicular transport processes in the cell[5,7–12]. BAR family of proteins have a wide range of curvatures with proteins such as F-Bar and N-BAR exhibiting positive curvatures[5,13] and proteins such as I-BAR exhibiting negative curvature[14]. When these proteins bind

to the membrane surface, they impose their local curvature on the membrane and also work in concert with each others at longer length scales to induce non-local curvatures on the membrane[15–19]. Though the sub-cellular processes of vesicular transports in mediated by multiple curvature proteins interacting in concert with each other, this aspect has not been studied very much in reconstitution experiments[20–24]. Also, a handful of theoretical and computational mesoscopic modeling work have provided important insights into the synergy between multiple scaffold proteins during membrane remodeling processes[25–28] but the studies are quite few in numbers and a more extensive exploration in this area is needed.

Also, lately role of flexible intrinsically disordered regions in scaffolding proteins has been shown to be important[29,30], which highlights the importance of considering the the effective curvature of the scaffold protein as a distribution rather than having one fixed curvature value. For example, BAR family protein Amphiphysin1 contains multiple disordered region[31] and Epsin N-terminal homology domain[32] as well as AP180 contains significant stretches of intrinsically disordered regions[32].

In this work, we develop a new framework to study multiple curvature proteins at mesoscopic scales. We use this framework to address the evolution of membrane morphologies as a function of mixture of differently curved proteins with different compositions and membrane binding strength as well as with a variety of protein-protein interactions behaviour. In our mesoscopic membrane mechanics based approach, we model the membrane as a triangulated surface and proteins as nematics. We use an augmented form of Helfrich type free energy function and perform Monte-Carlo simulations to model this process[33,34]. Membrane deformation with a single fixed scaffold protein is extensively studied by this method[33–36]. Here we have evolved the underlying Hamiltonian so that the method can be used to study membrane remodeling due to mixture of proteins with different curvatures working together.

II. MODEL

We model proteins as nematics and deformable fluid membrane as a triangulated surface. In this model[33,34], nematic lies on the local tangent plane of the vertex of the triangle. These nematics (proteins) are free to rotate in the local tangent plane and are denoted by $\hat{n}(\vec{r})$. Here, the interactions between protein and membrane are modelled as anisotropic

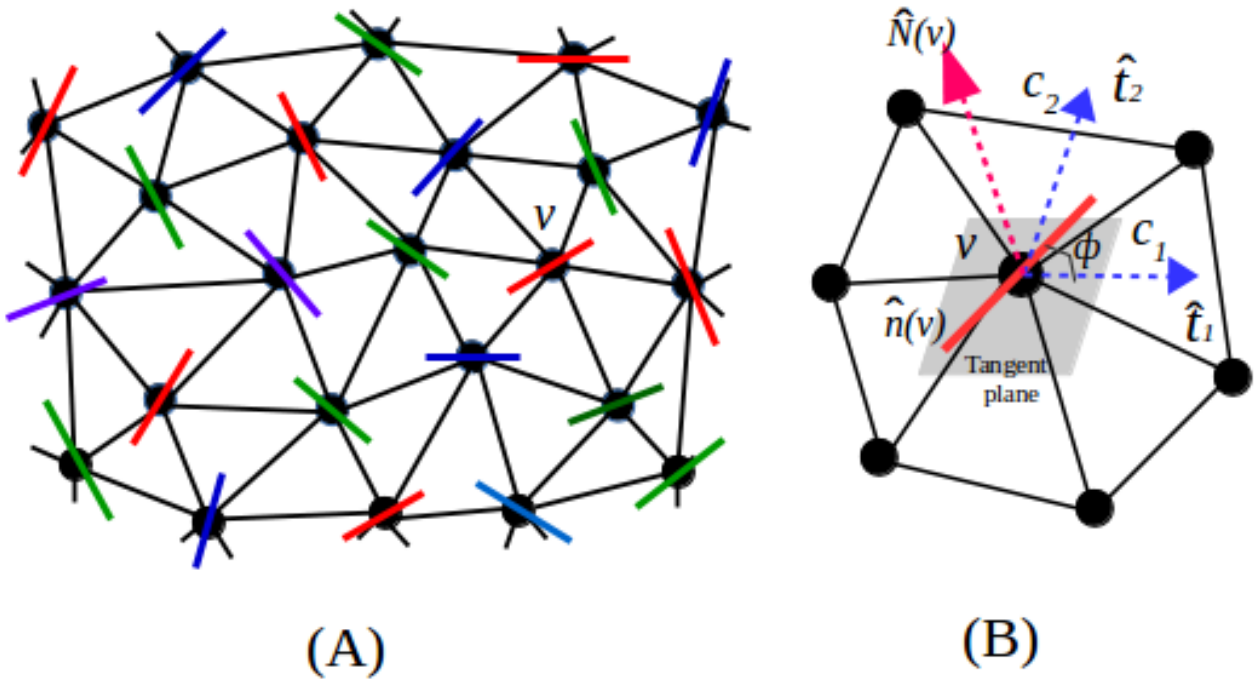

FIG. 1: Schematics for the model. (A) The triangulated mesh represents the elastic membrane sheet and the vectors on the nodes represent the proteins as in-plane nematics. The model can account for multiple types of nematics presented as different colors in the schematics. (B) The various geometric parameters in the models, elaborated below, are represented here.

spontaneous curvatures of the membrane in the vicinity of the protein filament. Protein-protein interactions are modelled by the splay and bend terms of the Frank's free energy for nematic liquid crystals. The total energy is the sum of membrane energy, energy due to interaction between protein and membrane and the protein-protein interaction energy. The energy of the bare membrane, which is the first of the total energy is written as:

$$E_1 = \frac{\kappa}{2} \int \Big(2H\Big)^2 dA$$

where E_1 is the Canham-Helfrich elastic energy for membranes[37,38], κ is bending rigidity and H is membrane mean curvature with $H = (c_1 + c_2)/2$. c_1 and c_2 are the local principal curvatures on the membrane surface along the orthogonal principal directions $\hat{t}_1$ and $\hat{t}_2$.

The coupling energy for the proteins and membrane interactions is written as E_2 below.

$$E_2 = \int \sum_{k=1}^{N} \Big(\frac{\kappa_{\|_k}}{2} (H_\| - c_{\|_k})^2 + \frac{\kappa_{\perp_k}}{2} (H_\perp - c_{\perp_k})^2 \Big) dA$$

Here, N is the number of different curvature values of proteins. $\kappa_\|$ and $\kappa_\perp$ are the induced membrane bending rigidities and $c_\|$ and $c_\perp$ are the induced intrinsic curvatures along $\hat{n}$ and $\hat{t}$. $\hat{n}$ is the orientation of the protein and $\hat{t}$ is its perpendicular direction in the local tangent plane. $H_\|$ and $H_\perp$ are the membrane curvatures in the direction of $\hat{n}$ and $\hat{t}$, where $H_\| = c_1 \cos^2\phi + c_2 \sin^2\phi$ and $H_\perp = c_1 \sin^2\phi + c_2 \cos^2\phi$. Here ϕ is the angle between the direction of nematic orientation $\hat{n}$ and the principal direction $\hat{t}_1$.

The protein-protein interactions is formulated as below:

$$E_3 = \int \sum_{k=1}^{N} \Big(\frac{K_1}{2} (\tilde{\nabla}.\hat{n})^2 + \frac{K_3}{2} (\tilde{\nabla}.\hat{t})^2 \Big) dA$$

E_3 is the energy for the nematic-nematic interactions and is modeled from the Frank's free energy for nematic liquid crystals. Here $\tilde{\nabla}$ is the covariant derivative on the curved surface. K_1 and K_3 are the splay and bending elastic constants for the in plane nematic interactions. Here, a discrete form of this energy is used[33] that makes the implementation amenable for the Monte-Carlo simulations and is expressed as:

$$E_3 = -\sum_{k=1}^{N} \epsilon_{LL}^{k,k} \sum_{i>j} \Big(\frac{3}{2} (\hat{n}_i.\hat{n}_j)^2 - \frac{1}{2} \Big)$$

The above formulation is inspired from the Lebwohl-Lasher model[39]. Here, ϵ_{LL} is strength of the nematic interaction with a constant approximation ($K_1 = K_3$). The sum $\sum_{i>j}$ is over all the nearest neighbour (i, j) vertices on the triangulated grid, promoting alignment among the neighbouring orientation vectors. Total energy is the sum of these three energy.

III. PARAMETERS

In this work, we use multiple curvature proteins with different densities and interactions. Below, we elucidate the input parameters used in the simulation for multiple curvature proteins expressed as matrices. If total number of different curvature proteins is N, then the nematic density is given as:

$$\rho = \begin{bmatrix} \rho_1 & \rho_2 & \dots & \dots & \rho_N \end{bmatrix} \text{ where } \sum_{i=1}^{n} \rho_i \leq n_v.$$

Here, $\rho_1, \rho_2, ...\rho_N$ are the densities of different curvature proteins(nematics) and n_v is the total number of the vertices on the triangulated surface. Here we have one nematic on every vertex. So the total number of nematics cannot exceed the total number of vertices. Different proteins can have different curvatures, induced membrane bending rigidities and interactions.

$$\kappa_{\parallel} = \begin{bmatrix} \kappa_{\parallel 1} & \kappa_{\parallel 2} & \dots & \dots & \kappa_{\parallel N} \end{bmatrix}$$
$$\kappa_{\perp} = \begin{bmatrix} \kappa_{\perp 1} & \kappa_{\perp 2} & \dots & \dots & \kappa_{\perp N} \end{bmatrix}$$
$$c_{\parallel} = \begin{bmatrix} c_{\parallel 1} & c_{\parallel 2} & \dots & \dots & c_{\parallel N} \end{bmatrix}$$
$$c_{\perp} = \begin{bmatrix} c_{\perp 1} & c_{\perp 2} & \dots & \dots & c_{\perp N} \end{bmatrix}$$

$\kappa_{\parallel 1}, \kappa_{\parallel 2}.....\kappa_{\parallel N}$ and $c_{\parallel 1}, c_{\parallel 2}.....c_{\parallel N}$ are the induced bending rigidities and curvatures of proteins along the direction of the nematics. $\kappa_{\perp 1}, \kappa_{\perp 2}.....\kappa_{\perp N}$ and $c_{\perp 1}, c_{\perp 2}.....c_{\perp N}$ are induced bending rigidities and curvatures in the perpendicular direction of nematics.

$$\epsilon_{LL} = \begin{bmatrix} \epsilon_{LL}^{1,1} & \epsilon_{LL}^{1,2} & \dots & \dots & \epsilon_{LL}^{1,N} \\ \epsilon_{LL}^{2,1} & \epsilon_{LL}^{2,2} & \dots & \dots & \epsilon_{LL}^{2,N} \\ \dots & \dots & \dots & \dots & \dots \\ \dots & \dots & \dots & \dots & \dots \\ \epsilon_{LL}^{N,1} & \epsilon_{LL}^{N,1} & \dots & \dots & \epsilon_{LL}^{N,N} \end{bmatrix}$$

Here $\epsilon_{LL}^{i,i}$ is the interaction between same curvature of nematics (same interaction) and $\epsilon_{LL}^{i,j}$ is the interaction between different curvature of nematics (cross interaction). We have

considered both cases $\epsilon_{LL}^{i,i} > \epsilon_{LL}^{i,j}$ and $\epsilon_{LL}^{i,i} < \epsilon_{LL}^{i,j}$ and show that how they affect the membrane deformation.

IV. RESULT AND DISCUSSION

In this work, our main focus is on the membrane remodeling due to mixture of different curvature proteins. We have also considered cases where a single protein can exist with variable curvatures due to fluctuations in the flexible regions of the proteins and we present such protein systems as a distribution of different curvatures. In all our simulations, the proteins are randomly distributed on the spherical vesicle in the initial setup and their organization and membrane deformation evolve and converge to the equilibrium solution. We have looked into the the protein organization and final vesicle shape due to interplay between proteins and membrane and we have also explored the factors leading to tubulation and membrane deformation that depend of non-local emergent factors such as bundling tendencies in proteins as well as curvature mediated protein organization and subsequent additional curvature formation. Before we move to salient findings of our studies, we present some simple cases that highlights the power of the method in studying curvature-proteins mediated membrane deformation in a high throughput manner.

Fig. 2 shows the vesicle deformation due to two different proteins with equal but opposite curvatures ± 0.5. The total protein coverage is 100% but densities of both proteins are changing regularly. On the x-axis, density of positively curved protein is decreasing from 90% to 10% while the density of negatively curved proteins in increasing from 10% to 90%. Protein-protein interaction is increasing along the y-axis. In Fig. 3(a-d), we show simulation results for the membrane remodeling due to two, three, four and five different curvature proteins. Fig. 3b-d with three, four and five different proteins have curvature values of $(0, \pm 0.5)$, $(\pm 0.5, \pm 0.8)$ and $(0, \pm 0.5, \pm 0.8)$, respectively. Here, the total protein coverage is 100%, which is equally divided into different curvature proteins. In these examples, we have taken bending rigidity of the membrane as $\kappa = 20K_bT$, induced bending rigidity as $\kappa_{\parallel} = 5K_bT$ and nematic-nematic interaction as $\epsilon_{LL} = 2K_bT$. In Fig. 4, we highlight how differential expression of proteins of different curvature affects membrane deformation. Fig.

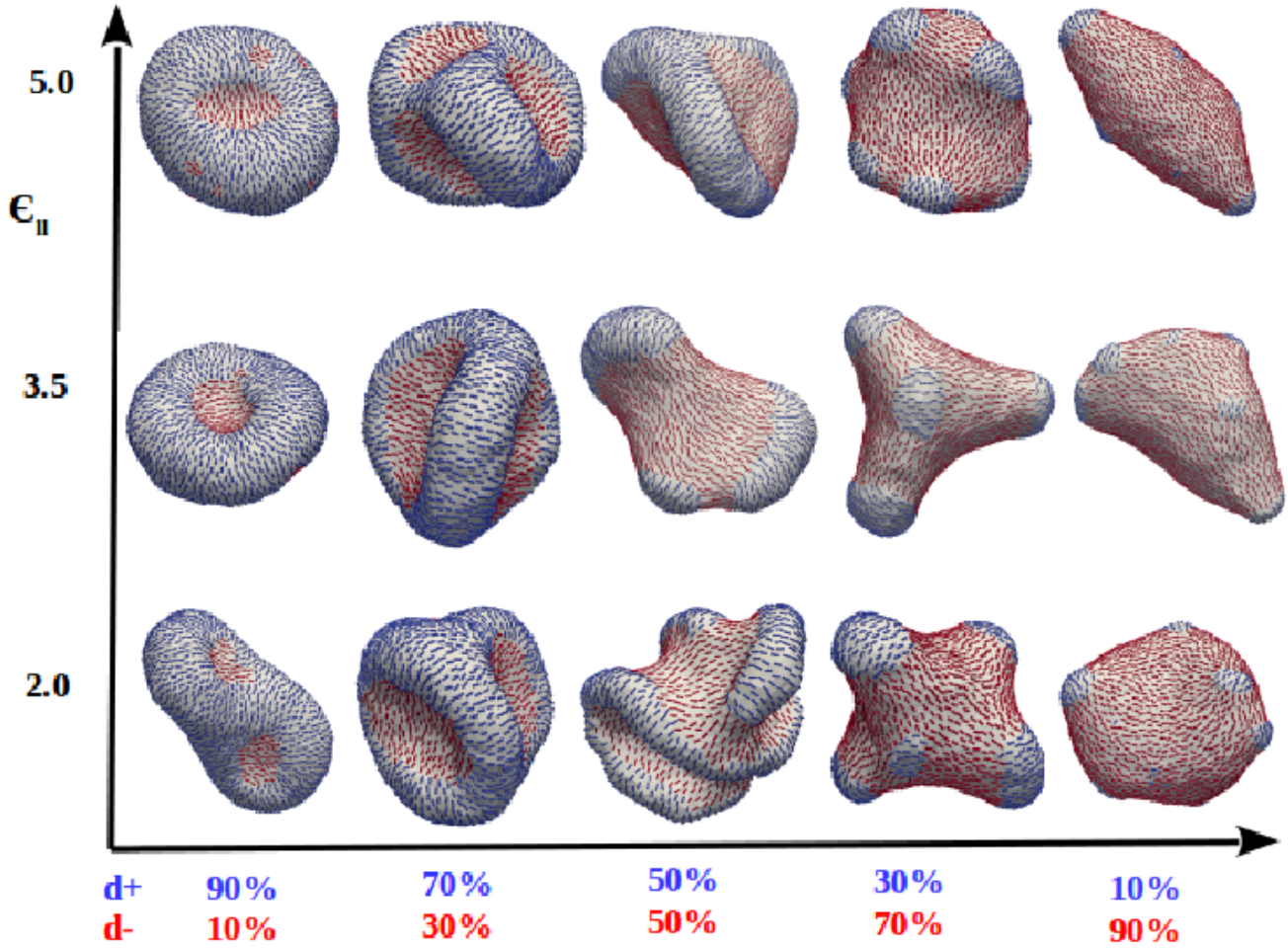

FIG. 2: Panel shows the vesicle deformation due to two different proteins with curvature (± 0.5). Here the different vesicle shapes are obtained with different proteins densities and different protein-protein interactions. On the X axis, density of positively curved protein is decreasing while negatively curved proteins in increasing. On the Y axis, nematic-nematic interaction in increasing. Other parameters are $\kappa = 20$, $\kappa_{\parallel} = 5$ in K_bT unit.

4 shows the vesicle deformation results due to three different curvature proteins where x-axis represents the densities of the different curvatures of proteins while y-axis represents protein-protein interaction. Different shapes are obtained due to different coverage ratio of curvature proteins and protein-protein interactions. In these results, the curvature of the proteins are $0.3, 0.4$ and 0.5 and the membrane-protein interaction $\kappa_{\parallel}$ is 10 K_bT. This example highlights the effect of up regulation or down regulation of certain protein on the overall membrane deformation. Together, these three examples highlight the capability of our model to studying membrane remodeling due to mixture of multiple types of curvature

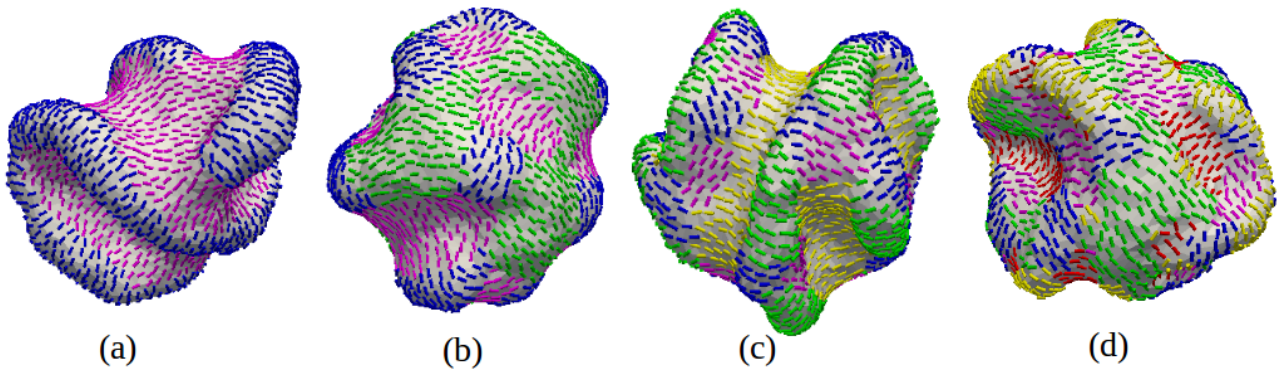

FIG. 3: Deformed vesicle morphologies obtained by Monte Carlo simulation. Panels shows the results for two, three, four and five different curvatures of proteins with curvature values (± 0.5), $(0, \pm 0.5)$, $(\pm 0.5, \pm 0.8)$ and $(0, \pm 0.5, \pm 0.8)$. Different colors show the different values of protein's curvature. Other parameters are $\kappa = 20$, $\kappa_{\parallel} = 5$ and $\epsilon_{LL} = 2$ in $K_b T$ unit.

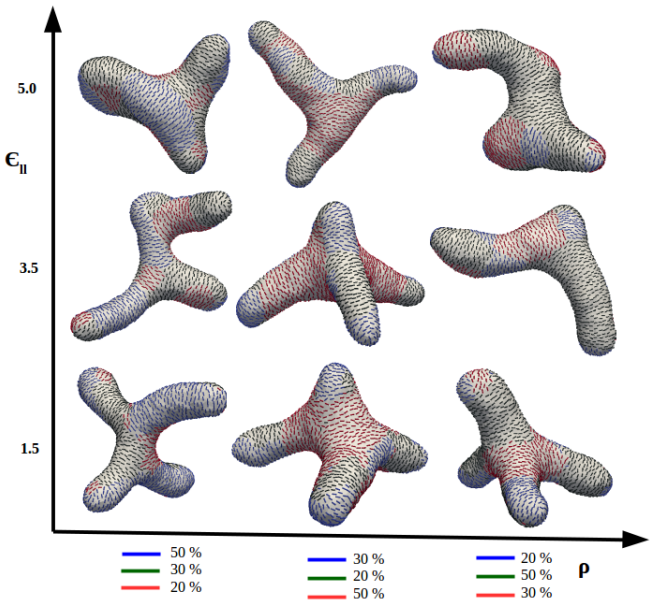

FIG. 4: Vesicle deformation due to three different curvature value of proteins. Different shapes are obtained by changing the densities of the different proteins and protein protein interaction. Other parameters are $\kappa = 20$, $\kappa_{\parallel} = 10$ in $K_b T$ unit.

proteins.

A. Weak interactions between protein types drive their demixing and induce non-local large membrane deformation

In cellular context, two or more different proteins frequently interact with each other during membrane remodeling processes[20–23]. However, due to the spatial and temporal resolution of the imaging techniques in membrane remodelling experimental studies, it is non-trivial to clearly observe the interplay between the proteins leading to membrane deformation. In this section, we show some simulation results where two different proteins having opposite curvatures come together for membrane deformation. We find that this does not always lead to membrane deformation. In particular, we focus on the factors that determine the localization and assembly patterns of the participating proteins leading to deformation. Fig. 5 shows the simulation results for two different curvature of proteins with different densities. Here the interaction between the different curvature proteins is also included and denoted by ϵ_{LL}^{Cross}. Protein coverage in upper and lower panels are 40% and 80%, respectively. Here the curvature of the two different proteins are ± 0.5. Proteins with positive curvature are shown by Blue color while the negatively curved proteins are shown by Red color. Fig. 5(a,d) shows the simulation result with $\epsilon_{LL}^{Cross} = 0$. Although there is no interaction between positively and negatively curved proteins, it is worth noting that they assemble as separate demixed groups in close proximity to each other. This is because positively curved proteins generate a negatively curved region on the bare membrane at the boundary of their local assembly and it is energetically most favorable for the negatively curved proteins to assemble in that region and stabilize the overall deformation profile. This is a clear example of curvature induced localization and assembly of second protein type. We also observe similar behavior in Fig. 3(a-d) where the proteins stabilize the final deformation by localizing in preferred curvature regions. We use Fig. 3b to accentuate the point here. Three different proteins with different curvatures are used in Fig. 3b. Blue and Pink nematics represent $+0.5$ and -0.5 curvatures, respectively while the Green represents 0.0 curvature. As is clear from the figure, the final deformed membrane has Blue nematics localizing on the positive outwards curvatures while the Pink nemantics populate the negative inwards curved part of the deformed vesicle. The Green nemantics, with zero curvature, are localized in the curvature regions between the other two. In Fig.

5(b,e), we keep the cross-interaction term $\epsilon_{LL}^{Cross} = 2$ such that $\epsilon_{LL}^{Cross} < \epsilon_{LL}$. As a result, the two protein are allowed to interact with each other but due to higher self-interaction, they tend to be demixed and localize in preferred curvature regions as in the first case. We also see that in Fig. 2, the different vesicle shapes are obtained due to different value of nematic-nematic interaction and different proteins density. It is worth noting that with increasing interactions, proteins with higher densities tend to assemble in one place rather than be localized in different pockets. This also leads to larger scale deformation rather than punctuated localized deformation. In systems with two proteins having equal and opposite curvatures, we find that a strong protein-protein interactions lead to complete mixing of the two kinds of proteins. In Fig. 5c,f, we modeled these situation where $\epsilon_{LL}^{Cross} > \epsilon_{LL}$. Due to the higher cross interactions, we observe that the two oppositely curvature proteins are arranged in random manner parallel to each other. The random arrangement of oppositely curved proteins in close proximity to each other has a compensatory effect on the curvature formation and no large scale curvature is visible.

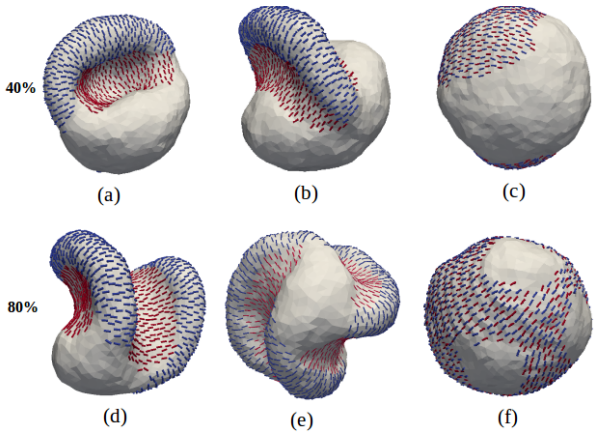

FIG. 5: Vesicle deformation results with non zero interactions between the two different curvature of proteins. Here density is fixed 40% for upper panel and 80% for lower panel. For (a,d) $\epsilon_{LL}^{Cross} = 0$ (b,e) $\epsilon_{LL}^{Cross} < \epsilon_{LL}$ (c,f) $\epsilon_{LL}^{Cross} > \epsilon_{LL}$.Other parameters are $\kappa = 20$, $\kappa_{\parallel} = 10$ and $\epsilon_{LL} = 3.5$ in K_bT unit.

Our simulations also provide some very interesting insights into cases with two different proteins having same curvature but different membrane protein interactions. This is important for many classes of curvature proteins including the various nexin complexes (SNXs) that have similar scaffold curvature but the membrane adaptor domains with preference for

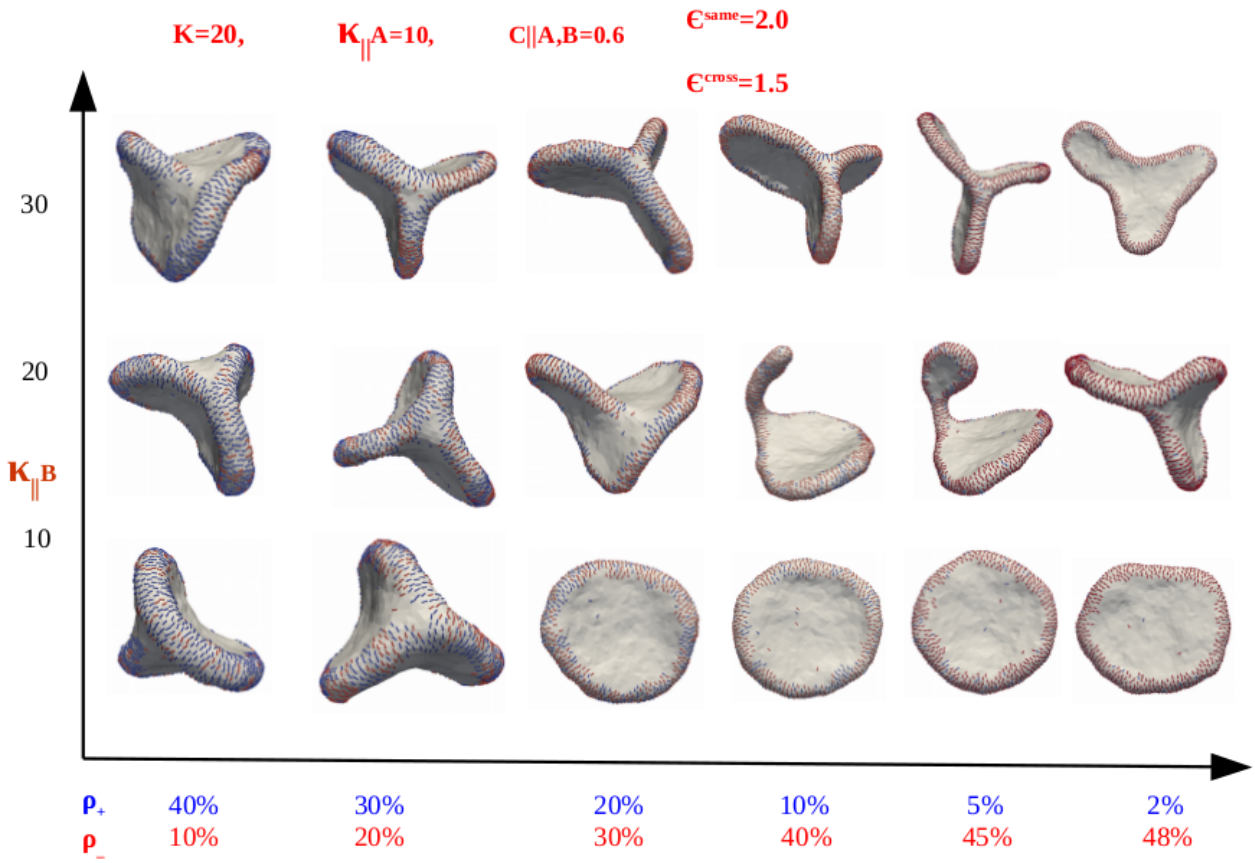

FIG. 6: Vesicle deformation due to two different proteins with equal curvature $c_{||} = 0.6$ and different membrane protein interactions. Other parameters are $\kappa = 20$, $\epsilon_{LL}^{same} = 2$ and $\epsilon_{LL}^{cross} = 1.5$ in K_bT unit.

certain organelle membranes. These proteins bind with different strength to a given membrane despite the same scaffold curvatures. Fig. 6 shows the membrane remodeling with two different proteins shown by Blue (A) and Red (B). We fixed the membrane-protein interaction of protein A to 10 K_BT and varied the membrane protein interaction of protein B, which is shown on the y-axis. The density of both proteins are changing on the x-axis but the total density is fixed and equal to 50%. Here, the protein-protein interaction between same proteins is 2 K_BT and in different proteins is 1.5 K_BT. We find that large membrane deformation as well as tubulation is possible is certain cases. In particular, we see tubulation when the density of tightly membrane bound proteins is 10% and loosely bound proteins is 40%. The membrane protein interaction of both proteins are 10 K_BT and 20 K_BT, respectively. Interestingly, in these systems, there is complete mixing between the proteins as

they prefer the same curvature, which suggest that assembly and localization of curvature proteins in not affected directly by how strongly they bind to the fluid membrane but by the strength of the protein-protein interactions. In the next section, we show the importance of protein-membrane interaction towards curvature formation.

B. Reticulation is facilitated by high membrane-protein interactions

Our analyses show that the strength of membrane protein interaction is the primary driving force for tubulation to occur. For example, in Fig.7, we present results for the vesicle deformation due to proteins with three different curvatures. Here protein curvatures are $0.5, 0.75$ and 1.0 with densities $30\%, 40\%$ and 30%, respectively. X axis shows increasing membrane protein binding interactions while the Y axis show an increasing protein protein interaction. As can be seen from Fig.7, different shapes are obtained due to different values of protein membrane interaction and protein protein interaction. We observe that the reticulaion propensity increases with the membrane protein interaction. For example, we see highly reticulated structures with thinner tubes for higher membrane protein interactions. This behavior is consistent across all protein-protein interactions, which suggests that though protein-protein interactions drive localization and certain degree of deformation, a high membrane protein interaction is required to induce large scaled tubulation profiles.

To highlight the dominant role of membrane-protein interaction over protein-protein interactions during tube generation process, we were able to create a case where tubes are formed from vesicle with two different proteins that are not interacting with each other at all. These results are presented in Fig. 8, where the total protein density is equal to 50% of the surface coverage but the ratio of protein densities is different in the four cases. The membrane protein interaction for tightly bound protein (shown in Red) and loosely bound proteins (shown in Blue) are 40 K_BT and 20 K_BT, respectively. All other parameters are same as for the system shown in Fig. 5.

Though protein-protein interactions are not the primary driving factor for large scale membrane deformation and tubulation, we find that presence of multiple scaffold protein

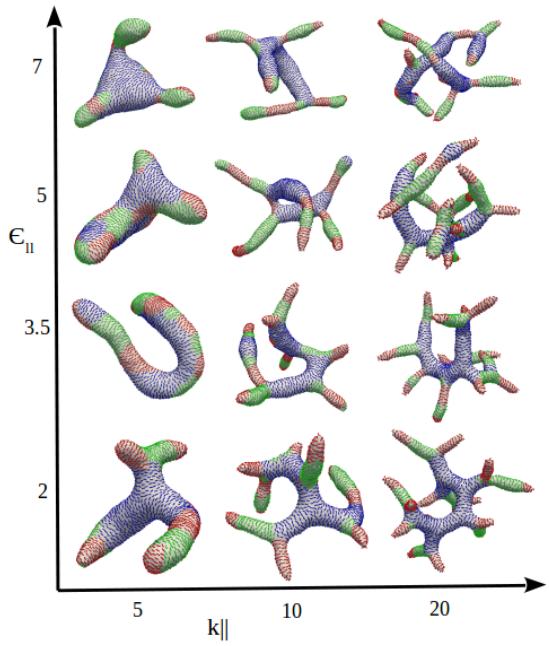

FIG. 7: Vesicle deformation due to proteins with three different curvature values $0.5, 0.75$ and 1.0 with protein coverage $30\%, 40\%$ and 30%. Different shapes are obtained due to different values of membrane nematic interaction and nematic-nematic interaction.

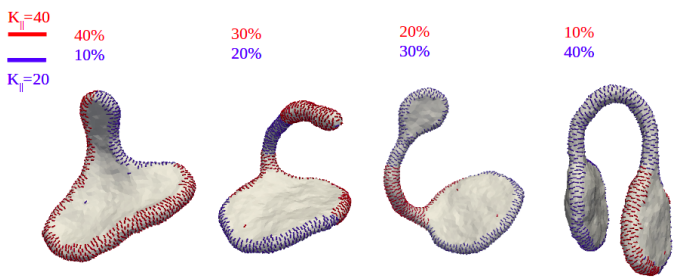

FIG. 8: Vesicle deformation due to two different proteins with equal curvature $c_{||} = 0.6$ and different membrane protein interactions. Other parameters are $\kappa = 20$, $\epsilon_{LL} = 2$ in K_bT unit.

tends to create tubulations or large deformation with overall less surface density than what can be achieved with a system with a single scaffold proteins. In Fig. 9, we show membrane remodeling due to one type of scaffold proteins. Here all parameters are same as Fig. 6. The protein density is varying on the x-axis and the membrane protein interaction is varying on the y-axis. It is clear from this figure that around 70% density of protein is required for the tubulation but we find in Fig. 6 that when two different proteins interact with the membrane, lesser overall surface density can cause tubulation (around 50%). The finding

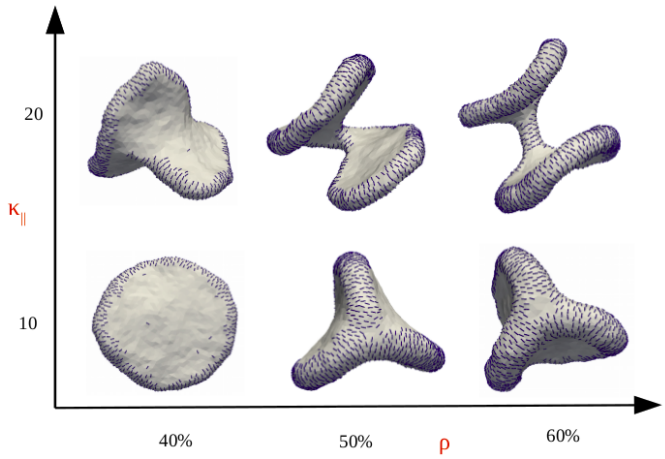

FIG. 9: Vesicle deformation due to one type of proteins with curvature $c_{||} = 0.6$ and Other parameters are $\kappa = 20$, $\kappa_{||} = 10$ and $\epsilon_{LL} = 2$ in K_bT unit.

that less protein density is required for membrane remodeling when two different proteins interact the membrane with different membrane protein interactions is quite interesting. We believe that presence of variety of curvature proteins allows the system to stabilize the evolving heterogeneous curvatures that occurs during the membrane remodeling process.

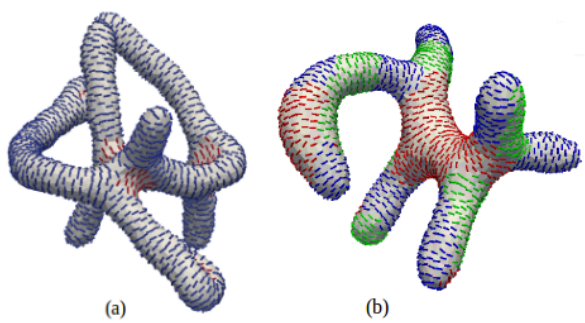

FIG. 10: (a) Membrane tubulation due to two different proteins with curvature 0.5 and -0.3. Positively curved proteins are stabilized on tube while the negatively curved proteins are stabilized at the junction between tubes. (b) Membrane tubulation due to proteins with variable curvature. Here the curvatures are 0.3, 0.4 and 0.5. Other parameters are $\kappa = 20$, $\kappa_{||} = 15$and $\epsilon_{LL} = 2$ in K_bT unit.

Endoplasmic reticulum (ER) like morphology is another another example where we find that the presence of mixed curvature protein systems is thermodynamically favorable to induce and maintain very thin reticulated structures with multiple complex junctions between tubules. In ER, tubes are stabilized by Reticulon and Reep proteins while the junction be-

tween them is stabilized by protein Lunapark. Fig. 10a shows the membrane tubulation with two different proteins with curvature 0.5 and -0.3. Positive curvature proteins form tube while the negative curvature proteins form the junction between the tubes. Here the protein density for positively and negatively curved proteins are 90% and 10% respectively. Other parameters are $\kappa = 20$, $\kappa_{\parallel} = 15$and $\epsilon_{LL} = 2$ in K_bT unit. Fig. 10b shows the membrane tubulation for different curvature values of two different proteins. Here the triple junction is forming like Endoplasmic reticulum. Positively curved proteins are forming the tubes while the negatively curved proteins are stabilizing at the junction. In heavily reticulated systems such as those belonging to ER and Golgi Apparatus, it is energetically more favorable to have a combination of positively and negatively curved scaffold proteins to stabilize a highly heterogeneous topology. Presence of one kind of scaffold protein leads to certain constraints that disallows morphologies like triple junction and neck regions where both positive and negative curvatures coexist and requires proteins with opposite curvature to stabilize such essential mixed curvature zones.

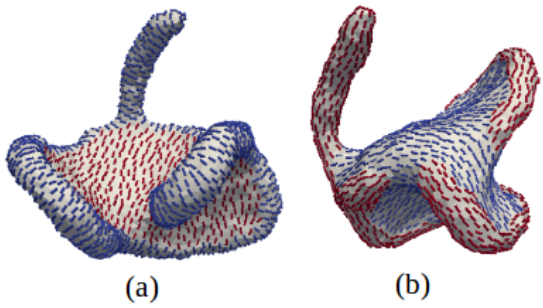

FIG. 11: Membrane tubulation due to two different proteins. (a) Both proteins are curved with curvature 1.0 (blue) and -0.05 (red) respectively. (b) one protein is curved with curvature -0.05 (blue) while the other one is straight $c_{\perp} = 1.0, c_{\parallel} = 0$ and have the tendency of bundle formation. Other parameters are $\kappa = 20$, $\kappa_{\parallel} = 10$, $\kappa_{\perp} = 10$ and $\epsilon_{LL} = 2$ in K_bT unit.

C. Zero curvature proteins can cause tubulations due to bundling tendencies

Membrane tubes are quite common in cell functions and are formed by the curved proteins and bundling tendency of the proteins. Tube formation due to bundling tendency of protein is briefly discussed in ref[34]. In this work, we show membrane tubulation due to

combination of two different curvature proteins. Fig.11a shows the membrane tubulation due to two curved proteins with curvature $c_{\parallel} = 1.0$ and -0.05. We show the positively curved proteins by Blue color those form the tube while the negatively curved proteins form valley and we show that by Red color. Proteins that don't have curvature but can form bundles like microtubule are also capable of creating membrane tubes. Fig.9b shows the membrane tubulation due to bundling of the proteins. Here one protein is has zero curvature (Red) $c_{\perp} = 1.0, c_{\parallel} = 0$ and another one have a positive curvature (Blue) $c_{\parallel} = -0.05$. Arrangement of the protein on the tube is different in Fig.9a and b. In Fig.11a, protein arrange themselves in the transverse direction to the length of the tube while in Fig.6a, they are along the length of the tube. This happens because in first case, tubulation occurs due to curved protein while in second case, bundling tendency of the proteins is the driver of tube formation.

V. CONCLUSION

Membrane deformation in cell occurs due to multiple proteins working in synergy with each other. Some processes like clathrin mediated endocytosis[4] and formation of three way junctions in the endoplasmic reticulum[40,41] are examples of membrane deformation and stabilisation of induced curvature due to multiple proteins. In this work, we have shown the deformation of membrane due to multiple proteins. These proteins can have different curvatures and interactions. We have included different values of the curvature and interaction and we also include the interaction between different curved proteins. From our Monte Carlo simulation results. we show that tubes are forming by positively curved proteins and valley (junction) are formed and stabilized by negatively curved proteins. We also show the effect of interaction between different curved proteins, where we report two particular cases: (i) $\epsilon_{LL}^{Cross} < \epsilon_{LL}$ and (ii) $\epsilon_{LL}^{Cross} > \epsilon_{LL}$. We show that the deformation occurs when $\epsilon_{LL}^{Cross} < \epsilon_{LL}$ between the two oppositely curved proteins. If the cross interaction is high ($\epsilon_{LL}^{Cross} > \epsilon_{LL}$), then no deformation occurs because in this case two oppositely curved proteins arrange at random position parallel manner. In this case, proteins are unable to deform the membrane. Further, we show that the membrane tubulation by the mixture of different proteins having a variety of curvatures leading to formation of different morphologies.

VI. AUTHOR CONTRIBUTIONS

Anand Srivastava conceived the idea and formulated the Hamiltonian with help of Gaurav Kumar. Gaurav Kumar wrote the software and carried out the simulations and all the analyses. Gaurav Kumar and Anand Srivastava wrote the paper.

VII. ACKNOWLEDGMENTS

Gaurav Kumar would like to acknowledge financial support from DST India, DBT-IISc and SERB. Financial support from the Indian Institute of Science-Bangalore and the high-performance computing facility "Beagle" setup from grants by a partnership between the Department of Biotechnology of India and the Indian Institute of Science (IISc-DBT partnership programme) are greatly acknowledged. A.S. thanks the startup grant provided by the Ministry of Human Resource Development of India and the early career grant from the Department of Science and Technology of India. A.S. also thanks the DST for the National Supercomputing Mission grant. FIST program sponsored by the Department of Science and Technology and UGC, Centre for Advanced Studies and Ministry of Human Resource Development, India is gratefully acknowledged by the authors. This research was also supported in part by the National Science Foundation under Grant No. NSF PHY-1748958 (KITP e-visit).

REFERENCES

[1]Carlo M Croce and George A Calin. mirnas, cancer, and stem cell division. *Cell*, 122(1):6–7, 2005.

[2]Harvey T McMahon and Emmanuel Boucrot. Molecular mechanism and physiological functions of clathrin-mediated endocytosis. *Nature reviews Molecular cell biology*, 12(8):517, 2011.

[3]Michael Mak, Fabian Spill, Roger D Kamm, and Muhammad H Zaman. Single-cell migration in complex microenvironments: mechanics and signaling dynamics. *Journal of biomechanical engineering*, 138(2), 2016.

[4]Marko Kaksonen and Aurélien Roux. Mechanisms of clathrin-mediated endocytosis. *Nature Reviews Molecular Cell Biology*, 19(5):313, 2018.

[5]JR van Weering, RB Sessions, C Traer, DP Kloer, VK Bhatia, D Stamou, SR Carlsson, JH Hurley, and PJ Cullen. In vitro snx-bar assembly reveals molecular details of distinct endosomal tubule formation. *EMBO J*, 31:4466–80, 2012.

[6]Michal Skruzny, Ambroise Desfosses, Simone Prinz, Svetlana O Dodonova, Anna Gieras, Charlotte Uetrecht, Arjen J Jakobi, Marc Abella, Wim JH Hagen, Joachim Schulz, et al. An organized co-assembly of clathrin adaptors is essential for endocytosis. *Developmental Cell*, 33(2):150–162, 2015.

[7]Brian J Peter, Helen M Kent, Ian G Mills, Yvonne Vallis, P Jonathan G Butler, Philip R Evans, and Harvey T McMahon. Bar domains as sensors of membrane curvature: the amphiphysin bar structure. *Science*, 303(5657):495–499, 2004.

[8]Jennifer L Gallop, Christine C Jao, Helen M Kent, P Jonathan G Butler, Philip R Evans, Ralf Langen, and Harvey T McMahon. Mechanism of endophilin n-bar domain-mediated membrane curvature. *The EMBO journal*, 25(12):2898–2910, 2006.

[9]Adam Frost, Vinzenz M Unger, and Pietro De Camilli. The bar domain superfamily: membrane-molding macromolecules. *Cell*, 137(2):191–196, 2009.

[10]Michitaka Masuda and Naoki Mochizuki. Structural characteristics of bar domain superfamily to sculpt the membrane. In *Seminars in cell & developmental biology*, volume 21, pages 391–398. Elsevier, 2010.

[11]Mijo Simunovic, Emma Evergren, Andrew Callan-Jones, and Patricia Bassereau. Curving cells inside and out: roles of bar domain proteins in membrane shaping and its cellular implications. *Annual review of cell and developmental biology*, 35:111–129, 2019.

[12]Natasza E Ziółkowska, Lena Karotki, Michael Rehman, Juha T Huiskonen, and Tobias C Walther. Eisosome-driven plasma membrane organization is mediated by bar domains. *Nature structural & molecular biology*, 18(7):854–856, 2011.

[13]Kohji Takei, Vladimir I Slepnev, Volker Haucke, and Pietro De Camilli. Functional partnership between amphiphysin and dynamin in clathrin-mediated endocytosis. *Nature cell biology*, 1(1):33–39, 1999.

[14]Pieta K Mattila, Anette Pykalainen, Juha Saarikangas, Ville O Paavilainen, Helena Vihinen, Eija Jokitalo, and Pekka Lappalainen. Missing-in-metastasis and irsp53 deform pi

(4, 5) p2-rich membranes by an inverse bar domain–like mechanism. *The Journal of cell biology*, 176(7):953–964, 2007.

[15]Thomas R. Weikl. Membrane-mediated cooperativity of proteins. *Annual Review of Physical Chemistry*, 69(1):521–539, 2018.

[16]Mijo Simunovic, Anand Srivastava, and Gregory A. Voth. Linear aggregation of proteins on the membrane as a prelude to membrane remodeling. *Proceedings of the National Academy of Sciences*, 110(51):20396–20401, 2013.

[17]Mijo Simunovic, Patricia Bassereau, and Gregory A Voth. Organizing membrane-curving proteins: the emerging dynamical picture. *Current Opinion in Structural Biology*, 51:99–105, 2018. Engineering and design: New applications • Membranes.

[18]Mijo Simunovic, Anela Šarić, J. Michael Henderson, Ka Yee C. Lee, and Gregory A. Voth. Long-range organization of membrane-curving proteins. *ACS Central Science*, 3(12):1246–1253, 2017.

[19]BJ Reynwar, G Illya, VA Harmandaris, MM Müller, K Kremer, and M. Deserno. Aggregation and vesiculation of membrane proteins by curvature-mediated interactions. *Nature*, (447):461–464, 2007.

[20]Zheng Shi. *Mechanisms of membrane remodeling by peripheral proteins and divalent cations*. PhD thesis, University of Pennsylvania, University of Pennsylvania, 2015.

[21]Adam Frost, Rushika Perera, Aurélien Roux, Krasimir Spasov, Olivier Destaing, Edward H Egelman, Pietro De Camilli, and Vinzenz M Unger. Structural basis of membrane invagination by f-bar domains. *Cell*, 132(5):807–817, 2008.

[22]Guillaume Drin and Bruno Antonny. Amphipathic helices and membrane curvature. *FEBS letters*, 584(9):1840–1847, 2010.

[23]Toshiki Itoh, Kai S Erdmann, Aurelien Roux, Bianca Habermann, Hauke Werner, and Pietro De Camilli. Dynamin and the actin cytoskeleton cooperatively regulate plasma membrane invagination by bar and f-bar proteins. *Developmental cell*, 9(6):791–804, 2005.

[24]Anne-Sophie Nicot, Anne Toussaint, Valérie Tosch, Christine Kretz, Carina Wallgren-Pettersson, Erik Iwarsson, Helen Kingston, Jean-Marie Garnier, Valérie Biancalana, Anders Oldfors, et al. Mutations in amphiphysin 2 (bin1) disrupt interaction with dynamin 2 and cause autosomal recessive centronuclear myopathy. *Nature genetics*, 39(9):1134–1139, 2007.

[25]Aram Davtyan, Mijo Simunovic, and Gregory A. Voth. The mesoscopic membrane with proteins (mesm-p) model. *The Journal of Chemical Physics*, 147(4):044101, 2017.

[26]Francesco Bonazzi, Carol K. Hall, and Thomas R. Weikl. Membrane morphologies induced by mixtures of arc-shaped particles with opposite curvature. *Soft Matter*, 17:268–275, 2021.

[27]Hiroshi Noguchi and Jean-Baptiste Fournier. Membrane structure formation induced by two types of banana-shaped proteins. *Soft Matter*, 13:4099–4111, 2017.

[28]Hiroshi Noguchi. Acceleration and suppression of banana-shaped-protein-induced tubulation by addition of small membrane inclusions of isotropic spontaneous curvatures. *Soft Matter*, 13:7771–7779, 2017.

[29]Wade F Zeno, Upayan Baul, Wilton T Snead, Andre CM DeGroot, Liping Wang, Eileen M Lafer, D Thirumalai, and Jeanne C Stachowiak. Synergy between intrinsically disordered domains and structured proteins amplifies membrane curvature sensing. *Nature communications*, 9(1):1–14, 2018.

[30]David J Busch, Justin R Houser, Carl C Hayden, Michael B Sherman, Eileen M Lafer, and Jeanne C Stachowiak. Intrinsically disordered proteins drive membrane curvature. *Nature communications*, 6(1):1–11, 2015.

[31]Natalia Pietrosemoli, Rita Pancsa, and Peter Tompa. Structural disorder provides increased adaptability for vesicle trafficking pathways. *PLoS Comput Biol*, 9(7):e1003144, 2013.

[32]Christoph Kalthoff, Jürgen Alves, Claus Urbanke, Ruth Knorr, and Ernst J Ungewickell. Unusual structural organization of the endocytic proteins ap180 and epsin 1. *Journal of Biological Chemistry*, 277(10):8209–8216, 2002.

[33]Netasan Ramakrishnan, PB Sunil Kumar, and John H Ipsen. Monte carlo simulations of fluid vesicles with in-plane orientational ordering. *Physical Review E*, 81(4):041922, 2010.

[34]Gaurav Kumar, N Ramakrishnan, and Anirban Sain. Tubulation pattern of membrane vesicles coated with biofilaments. *Physical Review E*, 99(2):022414, 2019.

[35]N. Ramakrishnan, P.B. Sunil Kumar, and Ravi Radhakrishnan. Mesoscale computational studies of membrane bilayer remodeling by curvature-inducing proteins. *Physics Reports*, 543(1):1–60, 2014. Mesoscale computational studies of membrane bilayer remodeling by curvature-inducing proteins.

[36]N Ramakrishnan, Ryan P Bradley, Richard W Tourdot, and Ravi Radhakrishnan. Biophysics of membrane curvature remodeling at molecular and mesoscopic lengthscales. *Journal of Physics: Condensed Matter*, 30(27):273001, jun 2018.

[37]Peter B Canham. The minimum energy of bending as a possible explanation of the biconcave shape of the human red blood cell. *Journal of theoretical biology*, 26(1):61–81, 1970.

[38]W Helfrich. Elastic properties of lipid bilayers: Theory and possible experiments. *Z. Naturforsch. C*, 28:693, 1973.

[39]PA Lebwohl. Pa lebwohl and g. lasher, phys. rev. a 6, 426 (1972). *Phys. Rev. A*, 6:426, 1972.

[40]Shuliang Chen, Tanvi Desai, James A McNew, Patrick Gerard, Peter J Novick, and Susan Ferro-Novick. Lunapark stabilizes nascent three-way junctions in the endoplasmic reticulum. *Proceedings of the National Academy of Sciences*, 112(2):418–423, 2015.

[41]Shuliang Chen, Peter Novick, and Susan Ferro-Novick. Er network formation requires a balance of the dynamin-like gtpase sey1p and the lunapark family member lnp1p. *Nature cell biology*, 14(7):707–716, 2012.